Characteristics of the Transition-State Spectra for ^{234}U, ^{236}U, and ^{240}Pu from (d,pf) and (t,pf) Angular-Correlation Experiments*

H. C. Britt, F. A. Rickey, Jr., and W. S. Hall
Los Alamos Scientific Laboratory, University of California, Los Alamos, New Mexico 87544
(Received 17 April 1968)

Fission-fragment angular correlations have been measured as a function of the excitation energy of the fissioning nucleus for the reactions ^{233}U(d,pf), ^{235}U(d,pf), ^{239}Pu(d,pf), and ^{234}U(t,pf). A simplified microscopic model is developed and used to fit the experimental results in the energy range up to the neutron binding energy. From these fits, the positions of vibrational bands with $K=0^+$, 2^+, 0^-, 1^-, and 2^- are determined for the transition-state spectrum of ^{234}U, ^{236}U, and ^{240}Pu. Above the neutron binding energy, the angular correlations are analyzed with a statistical model, and the pairing energy for a highly deformed transition nucleus is determined. Values obtained for the pairing gap are $2\Delta_0=2.10\pm0.15$ MeV for ^{236}U and $2\Delta_0=1.98\pm0.15$ MeV for ^{240}Pu.

I. INTRODUCTION

SINCE the concept of transition states for a fissioning nucleus was first introduced by A. Bohr,[1] there has been considerable interest in attempts to establish the existence and determine the properties of the lowest states in a variety of fissionable nuclei. Bohr[1] postulated that in the region of the saddle point, fission proceeds through definite transition states with well-defined quantum numbers. At excitation near the fission threshold it is expected that the nucleus will fission through only a few discrete transition states with the spectrum of low-lying states being similar to that observed for nuclei at their stable deformation. Near threshold the fission probability (or fission cross section) will be dependent on the positions of the first few transition states and the angular distribution of the fragments will be dependent on the angular momenta J and the projection of J on the nuclear symmetry axis K for the transition states involved. The first evidence for the existence of transition states came from studies of neutron resonance fission where fission width fluctuations indicated only a few open channels, and from structure observed in the fission cross section and angular distributions for neutron fission of even-even nuclei near threshold.[2] A review of the channel theory of fission and early experiments has been given by Wheeler.[3]

Studies of the properties of transition states are of current interest for several reasons. Gross properties of the transition states are important to the empirical analysis of fission cross sections. Detailed determinations of the energies for the low-lying transition states can provide tests for theoretical calculations of the potential energy of the nucleus as a function of deformation for very large deformations. A determination of the level structure at the fission saddle gives information on level systematics for a very deformed shape which can be compared with the level spectrum of the same nucleus at its equilibrium shape. Such a comparison involves only a change in nuclear deformation. This represents the only case where the effects due to changes of deformation can be uniquely separated from other nuclear effects.

One of the most promising techniques for investigating the properties of transition states is to observe the decay by fission of nuclei excited by a direct reaction. By measuring the energy of the outgoing direct particle in coincidence with fission, the properties of the fission de-excitation can be studied over a continuous region of excitation energies. Northrop *et al.*[4] used the (d,pf) reaction to make the first determination of the fission barriers of ^{234}U, ^{236}U, and ^{240}Pu. These results showed structure in the fission probability as a function of excitation energy which indicated the presence of low-lying vibrational states in the transition-state spectrum. More recently, measurements have been made on both fission probabilities and angular correlations for (d,pf),[5–9] $(\alpha,\alpha'f)$,[10,11] and (t,pf)[7,12] reactions. Many of these experiments have shown prominent structure in the dependence of both the fission probability and the angular correlations as a function of excitation energy near threshold. However,

* Work performed under the auspices of the U. S. Atomic Energy Commission.

[1] A. Bohr, in Proceedings of the First United Nations International Conference on the Peaceful Uses of Atomic Energy 1955, Vol. 2, p. 151 (unpublished).

[2] L. Wilets and D. M. Chase, Phys. Rev. **103**, 1296 (1956).

[3] J. A. Wheeler, in *Fast Neutron Physics, Part II*, edited by J. B. Marion and J. L. Fowler (Interscience Publishers, Inc., New York, 1963), Vol. II, p. 2051.

[4] J. A. Northrop, R. H. Stokes, and K. Boyer, Phys. Rev. **115**, 1277 (1959).

[5] H. C. Britt, W. R. Gibbs, J. J. Griffin, and R. H. Stokes, Phys. Rev. **139**, B354 (1965).

[6] R. Vandenbosch, J. P. Unik, and J. R. Huizenga, in *Proceedings of the Symposium on Physics and Chemistry of Fission* (International Atomic Energy Agency, Vienna, 1965), Vol. I, p. 547.

[7] H. C. Britt, R. W. Newsome, Jr., and R. H. Stokes, in *Symposium on Recent Progress in Nuclear Physics with Tandems* edited by W. Hering (Max Planck Institute for Nuclear Physics, Heidelberg, 1966).

[8] H. J. Specht, J. S. Fraser, and J. C. D. Milton, Phys. Rev. Letters **17**, 1187 (1966).

[9] K. L. Wolf, R. Vandenbosch, and W. D. Loveland, Phys. Rev. **170**, 1059 (1968).

[10] B. D. Wilkins, J. P. Unik, and J. R. Huizenga, Phys. Letters **22**, 243 (1964).

[11] H. C. Britt and F. Plasil, Phys. Rev. **144**, 1046 (1966).

[12] D. Eccleshall and M. J. L. Yates, in *Proceedings of the Symposium on Physics and Chemistry of Fission* (International Atomic Energy Agency, Vienna, 1965), Vol. I, p. 77.

the analysis of the results in terms of contributions from specific transition states has been inhibited by a lack of knowledge about the direct reaction used to excite the fissioning nuclei.

For odd neutron–even proton nuclei where the fission threshold is above the neutron binding energy there have been several recent experimental and theoretical studies of the structure in the fission cross section and angular distributions near threshold.[13–15] In the more recent of these studies[15,16] a realistic microscopic model has been used to try to determine the character and positions for the first few single particle transition states. The results show the necessity for analyzing cross sections and angular distributions simultaneously.

In the present experiments measurements have been made on the fission probability and the fragment angular correlation for the (d,pf) reaction on ^{233}U, ^{235}U, and ^{239}Pu and for the ^{234}U(t,pf) reaction. These results give information on the fissioning nuclei ^{234}U, ^{236}U, and ^{240}Pu, with ^{236}U being studied by both (d,pf) and (t,pf) reactions. For excitation energies below the neutron binding energy, the results are compared to detailed calculations for a simplified model of the direct-reaction fission process. From comparisons with calculated distributions the positions of the first few vibrational bands in the transition-state spectrum are determined. For excitations above the neutron binding energy, ^{234}U(t,pf) and ^{239}Pu(d,pf) results are analyzed with a statistical model and the pairing gap in the transition state spectrum is determined. ^{239}Pu(d,pf) measurements were made of the azimuthal angular correlation for the fragments at proton angles of 90°, 110°, and 130° to check the assumption[5] that the angular correlations can be described by a plane-wave theory.

II. EXPERIMENTAL PROCEDURE

A. General

The experiments were performed using 15.0- and 18.0-MeV deuteron and 18.0-MeV triton beams from the Los Alamos Scientific Laboratory Van de Graaff accelerator facility. A multipurpose scattering chamber was used which could accommodate a ΔE-E proton telescope and up to 8 independent fission detectors. Proton spectra were obtained in coincidence with each of the fission detectors yielding a full (up to 8 angles) angular correlation in a single run. In some cases, data were obtained for more than one fission detector configuration yielding angular correlations with more than 8 angles.

The ΔE detector was a 310-μ Au surface barrier, and the E detector was a lithium-drift detector of 2 or 3 mm thickness. The over-all resolution of the proton detection system was approximately 120 keV. The proton detector was collimated with a circular aperture and subtended an angle $\Delta\theta\sim15°$. The fission detectors were phosphorus-diffused semiconductor detectors of $\sim$400 Ω-cm silicon which were operated at reverse biases of 100–200 V. Detectors of two sizes were used, 8×8 mm square and 8×20 mm rectangular. For angles near the recoil angle, the square detectors were used and rectangular detectors were used for fission detectors that were nearly perpendicular to the recoil direction. In the reaction plane the fission detectors subtended an angle $\Delta\theta=13°$ for the (d,pf) measurements and $\Delta\theta=6.4°$ for the (t,pf) measurement.

The targets were prepared by vacuum evaporation on 40–80 μg/cm^2 carbon backings. The heavy elements were in the form of oxides with deposit thicknesses ranging from 100–300 μg/cm^2. The targets had isotopic compositions: ^{233}U—97.96%, ^{234}U—1.37%, ^{235}U—0.07%, ^{238}U—0.60%; ^{234}U—99.7%, ^{235}U—0.3%; ^{235}U—93.25%, ^{234}U—1.03%, ^{236}U—0.28%, ^{238}U—5.44%; and ^{239}Pu—94.41%, ^{240}Pu—5.23%, ^{241}Pu—0.36%.

B. Electronics and Data Acquisition

A schematic diagram of the data acquisition system used in these experiments is shown in Fig. 1. Pulses in the ΔE and E detectors are used in a multiplier-type particle identification system to isolate reaction protons from other light particles. The fission-proton coincidence system utilizes a time-to-height converter (THC) in a method similar to that described previously.[11] Fast signals are obtained from each fission detector and the ΔE detector using fast transformer pickoffs.[17] The mixed fission signals and the ΔE signals are sent to the two inputs of an overlap type THC. The analog output of the THC gives an approximately constant amplitude pulse for events in true coincidence and a uniform distribution of amplitudes for accidental events. When the coincidence requirements are satisfied, linear gates are opened and the analog THC and proton energy pulses are accepted by analog to digital converters at the interface of an SDS-930 computer. In addition, digital information is supplied to the computer for identification of the fission detector involved in a particular event. For primary data storage the computer writes the two pulse heights and the detector identification for each event on a magnetic tape. This tape is then used for the final data analysis at a later time. In addition, the computer does a limited analysis of the data to provide information necessary for judging the progress of the experiment. For each fission detector,

[13] R. W. Lamphere, Nucl. Phys. **38**, 561 (1962); and in *Proceedings of the Symposium on Physics and Chemistry of Fission* (International Atomic Energy Agency, Vienna, 1965), Vol. I, p. 63.

[14] P. E. Vorotnikov, S. M. Dubrovina, G. A. Otroshchenko, and V. A. Shigin, Yadern. Fiz. **3**, 479 (1966); **5**, 295 (1967) [English transls.: Soviet J. Nucl. Phys. **3**, 348 (1966); **5**, 207 (1967)]; P. E. Vorotnikov, Yadern. Fiz. **5**, 415 (1967) [English transl.: Soviet J. Nucl. Phys. **5**, 415 (1967)].

[15] R. Vandenbosch, Nucl. Phys. **A101**, 460 (1967).

[16] W. Loveland, J. R. Huizenga, A. Behkami, and J. H. Roberts, Phys. Letters **24B**, 666 (1967).

[17] ORTEC, Inc., Oak Ridge, Tennessee, Model 260.

a spectrum of the THC output is sorted. Then digital windows are set on the THC output corresponding to real and accidental coincidence events. Real and accidental proton-energy spectra are obtained and a coincidence proton-energy spectrum corrected for accidental contributions is generated for each fission detector.

The ratio of accidental to real events in the real window is in general quite small (5–10% except near the fission threshold). The precise method of correcting for accidental contributions results in the accuracy of the final results being determined entirely by statistical uncertainties and the determination of the relative solid angles of the detectors. The limiting factor in rate of data acquisition is the singles fission rate to the shaper preceding the THC. This shaper generates a 60-nsec pulse to the THC and has a characteristic dead time of ~300 nsec per event. In a typical experiment the beam was held to a level such that the dead time in this shaper was less than 5%. This limitation resulted in coincidence counting rates of ~5 events/sec in the (t,pf) experiment and ~25 events/sec in the (d,pf) measurements for an excitation energy range from threshold to ~5 MeV above threshold.

C. Data Analysis

The final data analysis is performed on a CDC 6600 computer using the event-by-event data which have been stored on magnetic tape. First, time spectra for each fission detector are sorted and optimum digital windows determined for real and accidental events. Then the real and accidental proton spectra in coincidence with each fission detector are sorted and a spectrum corrected for accidental contributions is generated. The corrected coincidence spectra are normalized to account for differences in the solid angles of the fission detectors and then each spectrum is converted to a new spectrum of number of counts versus excitation energy in the residual nucleus (fissioning nucleus) with standard channel widths of 50 keV. The conversion to an excitation energy spectrum involves a proton energy calibration of the ΔE-E system, the Q values of the reaction and a center-of-mass transformation to the rest system of the fissioning nucleus.[11] For each excitation energy interval the angle of each detector is calculated in the rest system of the fissioning nucleus (i.e., angle relative to kinematic recoil angle with center-of-mass correction). The statistical error on each point is also calculated.

For the above data reduction, the relative solid angles of the fission detectors are determined by comparing the relative singles fission rates with measured angular distributions for the appropriate (d,f) or (t,f) reaction. Relative solid angles determined in this manner were accurate to ±5%. The proton energy calibration of the ΔE-E system is determined from known energy proton groups for reactions on ^{12}C and ^{16}O. The reaction Q values were determined from (d,p) and (d,t) experiments[18,19] in the U isotopes and from mass tables[20] for the ^{239}Pu(d,pf) reaction. The Q values used are as follows: ^{239}Pu(d,p_0), Q_0=4.23 MeV; ^{233}U(d,p_0), Q_0=4.61 MeV; ^{235}U(d,p_0), Q_0=4.34 MeV; ^{234}U(t,p_0), Q_0=3.39 MeV.

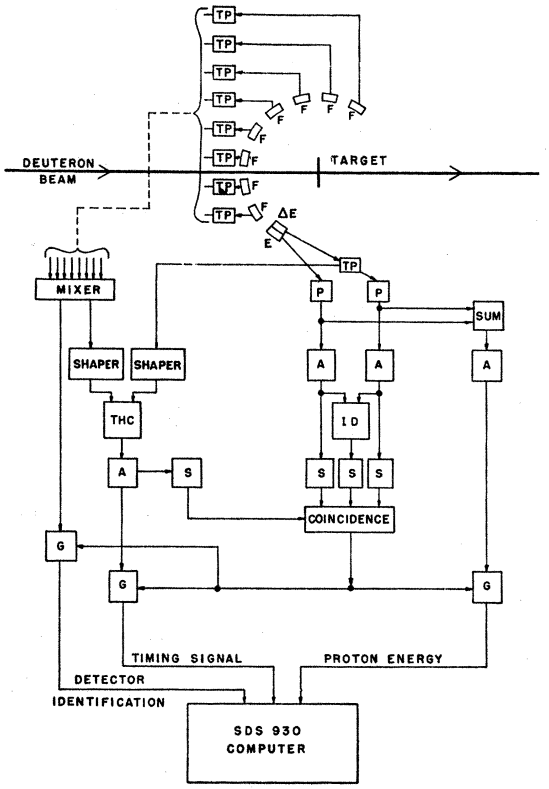

FIG. 1. A schematic diagram of the electronics apparatus. THC is time-to-pulse-height converter; A is linear amplifier; P is preamplifier; ID is analog particle identifier; TP is fast time pickoff; G is linear gate; S is single-channel analyzer.

For a given reaction, the data from all runs are combined into a single matrix of excitation energy and fission angle. Then at each excitation energy interval a least-squares fit is performed to the function

$$W(\theta)=A_0[1+\sum_{L=2,4,6\cdots} g_L P_L(\cos(\theta-\theta_0))],$$

where A_0, θ_0, and g_2, g_4, $\cdots$ were adjustable parameters, and the angles θ are measured in the rest system of the fissioning nucleus (i.e., relative to the kinematic recoil angle). In most cases, fits were first performed using all of the adjustable parameters. From these results an average value of θ_0 was determined and the final fits were obtained holding θ_0 fixed at its average value. The results gave average values of $\theta_0=0\pm2°$, indicating symmetry angles for the angular correlations that are

[18] J. R. Erskine, A. M. Friedman, T. H. Braid, and R. R. Chasman (to be published).
[19] F. A. Rickey, Jr., and H. C. Britt (to be published).
[20] J. H. E. Mattauch, W. Thiele, and A. H. Wapstra, Nucl. Phys. 61, 1 (1965).

TABLE I. Excitation energy intervals and parameters from the least-squares fit for Fig. 2.

	Reaction	Energy interval (MeV)	θ_0	g_2	g_4	g_6	g_8	g_{10}	g_{12}
A	$^{234}U(t,pf)$	5.22–5.57	1.4°	1.00±0.06	1.38±0.06	0.99±0.10	1.24±0.13	0.24±0.11	0.13±0.15
B	$^{234}U(t,pf)$	5.57–6.02	1.4°	1.14±0.03	1.33±0.05	1.09±0.05	1.16±0.07	0.38±0.06	0.23±0.08
C	$^{234}U(t,pf)$	6.22–6.42	1.4°	0.90±0.03	0.77±0.05	0.62±0.06	0.66±0.06	0.27±0.06	0.38±0.09
D	$^{234}U(t,pf)$	6.42–6.72	1.4°	0.82±0.03	0.68±0.04	0.41±0.05	0.34±0.06	0.18±0.05	0.21±0.07
E	$^{239}Pu(d,pf)$	4.87–5.22	0°	0.89±0.03	0.34±0.03	0.15±0.04	0	0	0
F	$^{239}Pu(d,pf)$	5.67–5.92	0°	0.53±0.02	0.18±0.02	0.03±0.02	0	0	0

coincident with the kinematic recoil angle to within the accuracy of the determination of the 0 of the angular scale.

For the (d,pf) reactions, the results were fit using terms up to P_6 in the above expression. For the (t,pf) reaction, terms up to P_{12} were required to fit the data near the fission threshold. The number of terms required for an acceptable fit to the experimental results was determined from the criterion that the weighted variance for an acceptable fit should be approximately equal to one. The experimental result and the fitted function are shown in Fig. 2 for several excitation energy intervals for the $^{234}U(t,pf)$ and $^{239}Pu(d,pf)$ results. For the (t,pf) results, the effect of the finite solid angle of the fission detectors was eliminated by fitting the results to the above expression integrated over the size of the detectors. In general, the correction for the finite solid angle of the detectors was less than the errors on the parameters. For the (d,pf) results, the solid-angle corrections were very small because of the less sharply peaked angular correlations (Fig. 2 and Table I) and have been neglected.

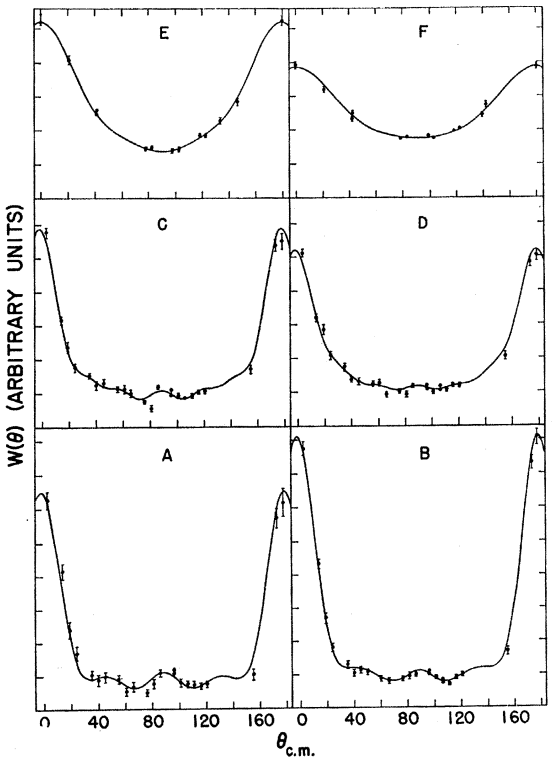

FIG. 2. Angular correlations with least-squares fits to Legendre polynomials for selected excitation energy intervals for the $^{234}U(t,pf)$ (A,B,C,D) and the $^{239}Pu(d,pf)$ (E,F) reactions. (Excitation energy intervals and parameters from the least-squares fit are given in Table I.) In all cases, the angular scale ($\theta_{c.m.}$) corresponds to angles in the rest system of the fissioning nucleus and the values of θ_0 were held fixed in the fitting procedure.

Finally, fission probability distributions P_f were determined for each case by converting the coefficients A_0 to a fission cross section σ_f, using measured absolute solid angles for the fission detectors and dividing by the singles proton cross section σ_s. In order to obtain σ_s, the contributions to the singles proton spectrum from carbon and oxygen contaminants in the targets had to be eliminated. The cross sections σ_s were obtained from singles spectra measured with a smaller aperture on the proton detector (to decrease kinematic broadening in the C and O peaks). In the region of contaminant peaks, the values for σ_s were obtained by a smooth extrapolation. The singles spectra used in the determination of σ_s are shown in Fig. 3. From the uncertainties in the absolute determination of σ_f and σ_s it is estimated that the uncertainty in the absolute values of the fission probabilities is ±10%.

III. EXPERIMENTAL RESULTS

A. $^{239}Pu(d,pf)$ Azimuthal Correlations

In the analysis of previous results[5,11] it has been assumed that the angular-correlation results can be theoretically described in terms of plane-wave angular correlations if the protons are observed at sufficiently large angles. Distorted-wave Born-approximation (DWBA) calculations for a variety of angular momentum transfers have shown the plane-wave approximation to be valid for $\theta_p > 120°$ for the (d,pf) reactions[5] and for $\theta_p > 75°$ for the $(\alpha,\alpha'f)$ reaction.[11] Consequences of the plane-wave assumption are that the angular correlations in the reaction plane are maximized and should be symmetric about the kinematic recoil angle and that the azimuthal (out-of-plane) angular correlations should be isotropic. These consequences have been experimentally verified previously for the $(\alpha,\alpha'f)$ reaction.[11]

In order to experimentally check the plane-wave assumption for the (d,pf) reactions, measurements were made for the $^{239}Pu(d,pf)$ reaction at 15.0-MeV

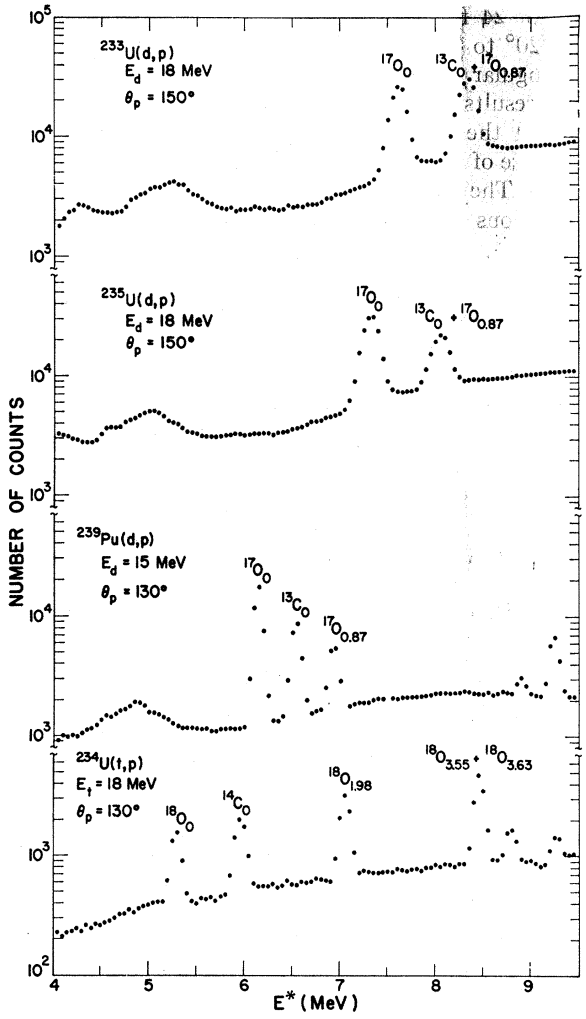

FIG. 3. Experimental singles proton spectra for the various energies and proton angles used in the coincidence experiments. Contaminant peaks from reactions on carbon and oxygen are labeled.

incident deuteron energy with 7 simultaneous fission angles both in and out of the reaction plane. Fission detectors were placed at angles (relative to the kinematic recoil angle) of $\theta=0°$, 20°, 40°, 90°, and 130° for $\phi=0°$, and at $\phi=45°$ and 90° for $\theta=90°$, where θ and ϕ refer to angles in the reaction plane and azimuthal angles, respectively. Measurements were made for proton angles of 90°, 110°, and 130°. The results of these measurements are shown in Fig. 4. The solid line in the g_2 distribution is simply a smooth curve through the $\theta_p=130°$ data presented below, which has much better statistical accuracy.

The results in Fig. 4 show that within the statistical accuracies the azimuthal distribution is isotropic for $\theta_p=110°$ and 130°, but for $\theta_p=90°$ the $W[(\phi=90°)/(\phi=0°)]$ ratio shows a significant deviation from isotropy. A more dramatic effect is apparent in the in-plane correlations where a significant decrease in g_2

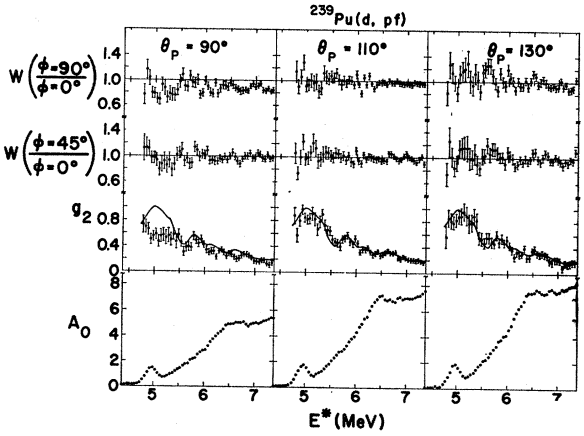

FIG. 4. Results of the azimuthal angular correlation experiments for ^{239}Pu(d,pf) at an incident deuteron energy of 15.0 MeV. The solid line in the in-plane correlation coefficients g_2 is a smooth curve through the more accurate experimental data shown in Fig. 10.

is seen near threshold for $\theta_p=90°$. In addition, the more detailed in-plane correlations for ^{239}Pu(d,pf) and ^{234}U(t,pf) at $\theta_p=130°$ (see Sec. III C below) indicate a symmetry angle consistent with the kinematic recoil angle for these two cases. These results are consistent with the (d,pf) calculations[5] which indicated the validity of the plane-wave approximation for $\theta_p>120°$.

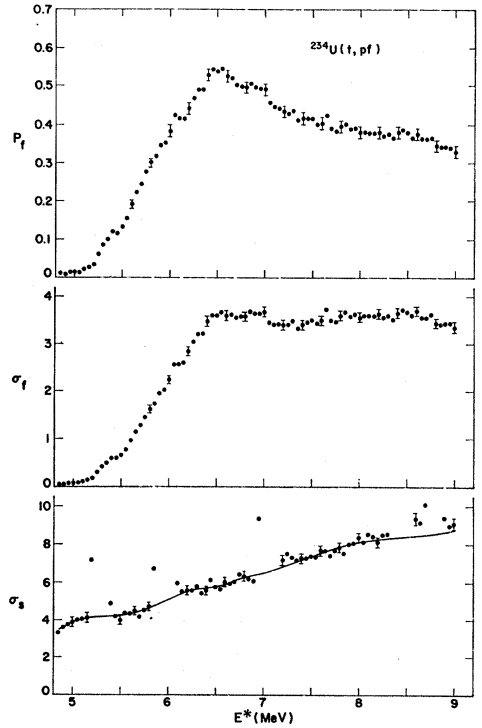

FIG. 5. Singles proton spectra (σ_s) and fission cross sections (σ_f) in arbitrary units. Resultant fission probability for the ^{234}U(t,pf) reaction. Solid curve in σ_s is an extrapolation underneath carbon and oxygen peaks which was used to determine P_f as described in the text.

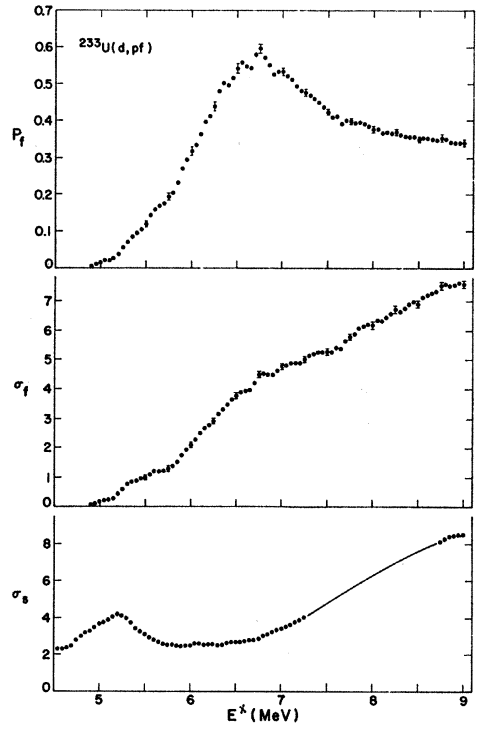

FIG. 6. Singles proton spectra (σ_s) and fission cross sections (σ_f) in arbitrary units. Resultant fission probability for the $^{233}U(d,pf)$ reaction. Solid curve in σ_s is an extrapolation underneath carbon and oxygen peaks which was used to determine P_f as described in the text.

Similar results and conclusions have been obtained by Wolf *et al.*[9] for the $^{239}Pu(d,pf)$ reaction at 15.0 MeV.

B. Fission Probabilities

For the four reactions, fission probabilities were obtained from $P_f=\sigma_f/\sigma_s$, where σ_f is obtained from the leading term A_0 in the fit to the angular correlations and σ_s is the singles proton distribution corrected for carbon and oxygen contaminant peaks. The dependence on excitation energy for σ_f, σ_s, and P_f are shown in Figs. 5–8 for the four cases studied. The singles spectra σ_s are also shown in Fig. 3 before corrections are made for the contributions from ^{12}C and ^{16}O reactions. The relatively slow variation of σ_s with E^* justifies the extrapolation procedure used for eliminating carbon and oxygen peaks from the spectra.

C. Angular Correlations

As described in the previous section, the fission fragment angular correlations were fit to a function $W(\theta)=A_0[1+\sum_L g_L P_L(\cos(\theta-\theta_0))]$. The experimental configuration and results obtained for each reaction are as follows.

1. $^{234}U(t,pf)$, $E_t=18.0$ *MeV*, $\theta_p=130°$, $\theta_{Recoil}\sim 15°$

In this experiment, data were taken for three separate configurations of eight fission detectors. This gave a total of 24 fission angles placed at laboratory angles from 20° to 195°. The fits gave a symmetry angle for the angular correlation $\theta_0=\theta_{sym}-\theta_R=-1.4\pm 2°$. For these results, terms up to $P_{12}(\cos\theta)$ were used in the fits and the fitting procedure was corrected for the finite size of the detectors as described in the preceding section. The final results are shown in Fig. 11. Angular correlations for selected energy intervals are shown in Fig. 2.

2. $^{239}Pu(d,pf)$, $E_d=15.0$ *MeV*, $\theta_p=130°$, $\theta_R\sim 20°$

Data were taken in two separate fission detector configurations for a total of 13 fission angles. The fission angles were spaced in the range of laboratory angles $-80°$ to $+200°$. The fits gave a symmetry angle $\theta_0=0°\pm 2°$. In this case, only terms up to $P_6(\cos\theta)$ were needed in the fits and no corrections were made for the finite size of the detectors. The final results are shown in Fig. 12. Angular correlations for selected energy intervals are shown in Fig. 2. Coincidence spectra near 0° and 90° in the rest system of the fissioning nucleus and experimental anisotropies for this reaction are shown in Fig. 9. It should be noted that the anisotropies are obtained from only a fraction of the data in the angular correlations so that statistical accuracies are somewhat poorer than in the results presented in Fig. 12.

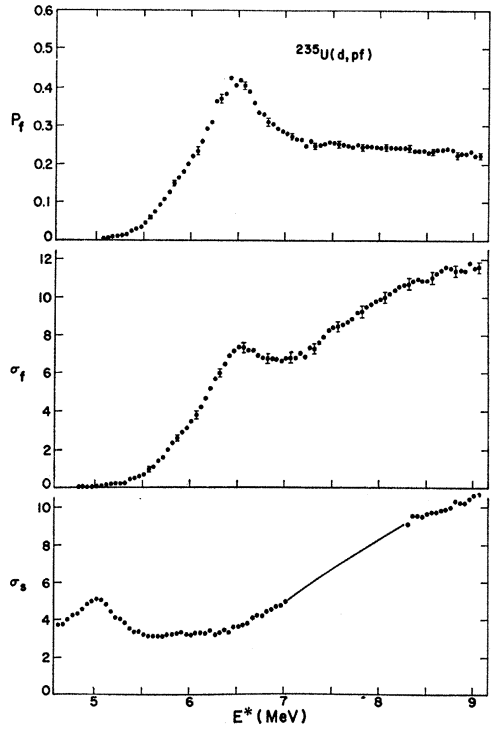

FIG. 7. Singles proton spectra (σ_s) and fission cross sections (σ_f) in arbitrary units. Resultant fission probability for the $^{235}U(d,pf)$ reaction. Solid curve in σ_s is an extrapolation underneath carbon and oxygen peaks which was used to determine P_f as described in the text.

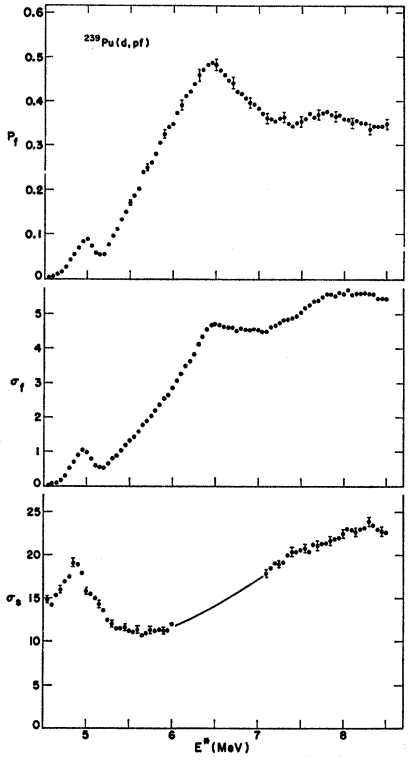

FIG. 8. Singles proton spectra (σ_s) and fission cross sections (σ_f) in arbitrary units. Resultant fission probability for the ^{239}Pu(d,pf) reaction. Solid curve in σ_s is an extrapolation underneath carbon and oxygen peaks which was used to determine P_f as described in the text.

3. $^{233}U(d,pf)$ and $^{235}U(d,pf)$, $E_d=18.0$ MeV, $\theta_p=150°$, $\theta_R\sim12°$

In these measurements, one experimental configuration of seven fission detectors was used. The fission detectors were at laboratory angles from 20° to 160°. Because of the less distinctive angular correlations and the smaller number of fission angles, it was not possible to determine a symmetry angle from the data. $\theta_0=0°$ was assumed. The data were fit with terms up to $P_6(\cos\theta)$ but the P_6 coefficients were very small. P_2 and P_4 coefficients are shown in Figs. 13 and 14 for the two cases. Coincidence spectra near 0° and 90° in the rest system of the fissioning nucleus and experimental anisotropies for these reactions are shown in Fig. 10. It should be noted that the anisotropies are obtained from only a fraction of the data in the angular correlation so that statistical accuracies are somewhat poorer than in the results present in Figs. 13 and 14.

IV. ANALYSIS OF RESULTS: MODEL FOR $E^*<B_n$

A. Method and Assumptions for Model

In order to attempt to identify the low-lying vibrational bands in the transition-state spectrum, calculations have been performed with a simplified model

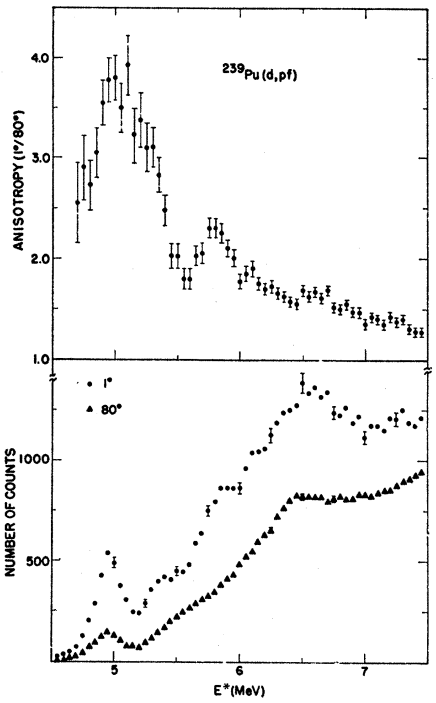

FIG. 9. Coincidence spectra for fission detectors at angles of 1° and 80° and the anisotropies (ratio 1°/80°) obtained from these spectra for the ^{239}Pu(d,pf) reaction. The data have been transformed to the rest system for the fissioning nucleus.

and the results compared to the observed P_f and g_L distributions. In general, very little quantitative information is available on the detailed characteristics of the levels excited in the direct reaction as a function of angular momentum, parity, and excitation energy. Similarly, only limited information is available on the fission and γ-ray widths which govern the decay of the

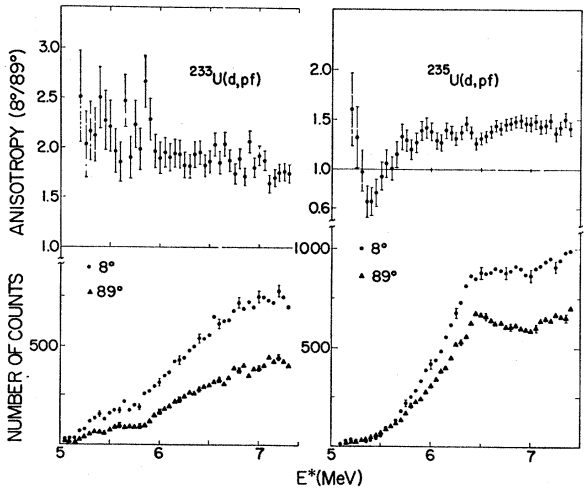

FIG. 10. Coincidence spectra for fission detectors at angles of 8.5° and 89° and the anisotropies (ratio 8.5°/89°) obtained from these spectra for the ^{233}U(d,pf) and ^{235}U(d,pf) reactions. The data have been transformed to the rest system for the fissioning nucleus.

residual nucleus excited by the direct reaction. However, the experimental results represent averages over all angular momentum and parity states and near the fission threshold the onset of fission through new vibrational bands produces very distinctive changes in the P_f and g_L distributions. Therefore, it was hoped that with a qualitative average model of the formation and decay processes it would be possible to identify the positions of the low-lying vibrational bands in the transition-state spectrum even though the formation and decay processes are not understood in complete detail. In addition, comparisons of the simplified model to experimental results can be used to gain the insight necessary for developing a more realistic model of the direct-reaction fission process. The qualitative features and assumptions of the calculations are as follows.

1. Formation Process

Average direct-reaction cross sections are used to describe the relative probability of various orbital angular momentum transfers, and it is assumed that these relative cross sections are independent of the excitation energy in the residual nucleus over the range of interest (4.5–8 MeV). In general, direct reactions predominantly excite particular classes of states (single-neutron states for the d,p reactions and two-quasiparticle states for the t,p reaction). At excitation energies of 4–8 MeV, the density of levels in the residual nucleus is very high so that states of a particular character, such as single-neutron states, are strongly mixed with the background of more complex states which have the appropriate spin and parity. This mixing is evident in the cross sections for both the (d,p) and (t,p) reactions, which indicate a smooth variation of the proton spectrum in the excitation energy region of interest. Some assumptions must be made about the distribution of states of the appropriate type which are available. In the simplified model it is assumed that the angular momentum distribution of states, $\rho(J^\pi)$, available for excitation in the residual nucleus is of a statistical form with one adjustable parameter which is used to obtain an empirical description of the spectrum of states excited. The formation cross sections and the statistical distribution of states is then used to obtain an average population $N(J^\pi)$ for states in the residual nucleus.

2. Decay Process

For each possible final angular momentum and parity in the residual nucleus the competition between fission and γ-ray de-excitation is calculated. The γ width Γ_γ is assumed to be independent of excitation energy, angular momentum, and parity. The fission widths $\Gamma_f(J^\pi)$ are calculated using a statistical level density and an assumed distribution of vibrational bands in the transition-state spectrum. Fission widths are calculated assuming penetration through a parabolic fission barrier which has the same shape for all angular momenta and both parities. From $\langle\Gamma_f(J^\pi)\rangle$ and Γ_γ the average fission probability $P_f(J^\pi)$ is calculated assuming a Porter-Thomas distribution[21] of fission widths with the appropriate number of degrees of freedom.

3. Final Fission Distribution

The final probability of fission, $P_f(E^*)$, is obtained at each excitation energy by taking an average over all states of $P_f(J^\pi)$ weighted by the populations of the states $N(J^\pi)$. For a particular J^π, angular correlation coefficients $g_L(J^\pi)$ are calculated as a function of the excitation energy of the residual nucleus assuming a plane-wave approximation.[5] Then the final coefficients $g_L(E^*)$ are obtained by taking a weighted average over all the states, $N(J^\pi)$, for each excitation energy interval. To compare with experimental data all calculations are performed at 50-keV intervals over the region of excitation energy of interest for a particular case.

4. Variable Parameters

The transition-state spectrum is defined by the positions of the lowest member for each vibrational band and the character $(J^\pi K)$ for each state. A barrier penetrability coefficient $\hbar\omega$ and a rotational constant E_R are assumed. In addition, several parameters are included which relate to the formation and decay of the compound states. They are (a) a level density parameter a used in the description of the dependence of Γ_f on excitation energy, (b) a spin cutoff factor s used in the dependence of Γ_f on angular momentum and in the density of states available to the direct reaction, (c) a parameter P that gives the ratio of negative parity to positive parity level densities in the residual nucleus, and (d) the absolute value for Γ_γ.

B. Detailed Calculations

In this section, a detailed description will be given of the calculations outlined in the preceding section. Average cross sections for specific angular momentum transfers, $\sigma(l)$ were obtained from DWBA calculations using the code JULIE[22] for the (d,p) reaction at 15 and 18 MeV and for the (t,p) reaction at 18 MeV. The optical parameters were obtained from fits to triton, deuteron, and proton elastic scattering on ^{234}U with the code PEREY.[23] The parameters used are listed in Table II and details of their determination will be given in a subsequent paper.[19]

For the (d,p) reaction, the distribution of states excited as a function of angular momentum is obtained

[21] C. E. Porter and R. G. Thomas, Phys. Rev. **104**, 483 (1956).
[22] We are indebted to R. M. Drisko and R. H. Bassel, Oak Ridge National Laboratory, for supplying us with a copy of this code.
[23] C. M. Perey, Phys. Rev. **131**, 745 (1963); C. M. Perey and F. G. Perey, *ibid.* **132**, 755 (1963).

TABLE II. Optical-model parameters used in DWBA calculations of relative $f(l)$'s. Notation is that of Perey and Perey (Ref. 23).

Particle	V_s (MeV)	r_{0s} (F)	a_s (F)	W_d (MeV)	W_s (MeV)	r_{0I} (F)	a_I (F)
Proton	50.13	1.25	0.71	13.05	0.0	1.25	0.78
Deuteron	76.6	1.30	0.78	22.9	0.0	1.34	0.69
Triton	168.3	1.24	0.684	0.0	14.52	1.45	0.987

$Q(d,p)=0.0$, $Q(t,p)=-2.0$

as follows for a target of spin I_0. The cross section for stripping a neutron to a particular orbital (j^π) is

$$\sigma(j^\pi)=\sigma(l=j\pm\tfrac{1}{2}),$$

where π refers to the two possible parities determined by l even or odd. It is assumed that each l transfer contributes equally to the two possible j states and thus a complete set of $\sigma(j^\pi)$ is generated. The cross section for exciting a particular final state (J^π) in the residual even-even nucleus is then given by

$$\sigma(J^\pi)=(2J+1)\sum_{j=|J-I_0|}^{J+I_0}\left(\frac{\sigma(j^\pi)}{(J+I_0)-|J-I_0|}\right).$$

Finally, the distribution of states excited in the residual nucleus is taken as

$$N(J^\pi)=\sigma(J^\pi)\rho(J^\pi),$$

where $\rho(J^\pi)$ is a statistical spin density function

$$\rho(J^\pi)=(2J+1)\{\exp[-J(J+1)/2s^2]\}P(\pi),$$

where s is the standard spin cutoff factor and $P(\pi)$ is an adjustable parameter which describes the relative density of positive and negative parity levels in the residual nucleus [$P(+)=1$ and $P(-)$ is variable].

For the (t,p) reaction, it is assumed that two neutrons coupled to angular momentum 0 are transferred so that

$$\sigma(J^\pi)=\sigma(l=J).$$

In this approximation, the (t,p) reaction can excite only natural parity states (even J for + parity; odd J for − parity).

In the next step of the calculations, a spectrum of transition states is generated by assuming a series of vibrational bands defined by an excitation energy E_i^*, the projection of the total angular momentum on the symmetry axis, K_i, and the parity of the band π_i. For each band, a spectrum of levels is generated from

$$E_i^*(J)=E_i^*+[J(J+1)-K_i^2]E_R,$$

where the rotational energy constant E_R is assumed to be the same for all bands.

With this spectrum of transition states average fission widths can be calculated as a function of excitation energy:

$$\langle\Gamma_f(E^*J^\pi)\rangle=[1/2\pi\rho(E^*J)]\nu_f(E^*J^\pi),$$

where $\nu_f(E^*J^\pi)$ is the effective number of open fission channels of a particular type, J^π. If the fission barrier is assumed to have a parabolic shape,[24]

$$\nu_f(E^*J^\pi)=\sum_i\{1+\exp(2\pi/\hbar\omega)[E_i^*(J^\pi)-E^*]\}^{-1},$$

where the sum is over all the transition states with character J^π and the curvature of the barrier is described by the parameter $\hbar\omega$.

The level densities $\rho(E^*J)$ were taken of the form given by Gilbert and Cameron[25]

$$\rho(U,J)=\frac{\sqrt{\pi}}{12}\frac{\exp[2(aU)^{1/2}]}{a^{1/4}U^{5/4}}\times\frac{(2J+1)\exp[-(J+\frac{1}{2})^2/2s^2]}{2(2\pi)^{1/2}s^3},$$

where $U=E^*-P(N)-P(Z)$.

$P(N)$ and $P(Z)$ are tabulated[25] pairing energy corrections. Values were also given[25] for the parameters a and s, but it was found that different values were needed to reproduce the experimental results, so that a and s were treated as adjustable parameters, and $\rho(U,J)$ renormalized to give the measured average level spacings from neutron resonance experiments. At excitation energies below the neutron binding energy, only fission and γ-ray de-excitation are allowed, so that for each J^π, the fission probability is given by

$$P_f(E^*J^\pi)=\left\langle\frac{\Gamma_f(E^*J^\pi)}{\Gamma_f(E^*J^\pi)+\Gamma_\gamma}\right\rangle,$$

where the average is taken assuming the Γ_f values are distributed according to a Porter-Thomas distribution[21] with the appropriate number of degrees of freedom.[26] The average fission probability is given by

$$P_f(E^*)=\sum_{J^\pi}P_f(E^*J^\pi)N(J^\pi)/\sum_{J^\pi}N(J^\pi).$$

The angular correlations have been parametrized in the form

$$W(\theta,E^*)\propto 1+\sum_L g_L(E^*)P_L(\cos\theta)$$

and in the model the coefficients $g_L(E^*)$ $(L=2, 4, 6, \cdots)$ are calculated. Following the previous theoretical development[5] for the (d,pf) reaction (see Sec. III A), it is assumed that for a specific l transfer, the angular correlations can be described by a plane-wave theory. For the (d,pf) reaction this gives the form

$$W_{jJI_0K}(\theta)\propto 1+\sum_L g_L(jJI_0K)P_L(\cos\theta)$$

for a (d,p) reaction to a particular neutron orbital j

[24] D. L. Hill and J. A. Wheeler, Phys. Rev. 89, 1102 (1953).
[25] A. Gilbert and A. G. W. Cameron, Can. J. Phys. 43, 1446 (1965).
[26] For each case the number of degrees of freedom was determined from ν_f. If $\nu_f<1$, one channel was assumed. If $1<\nu_f<2$, calculations were performed for one fully open channel plus one partially open channel. For $\nu_f>2$, two fully open and one partially open channel were assumed.

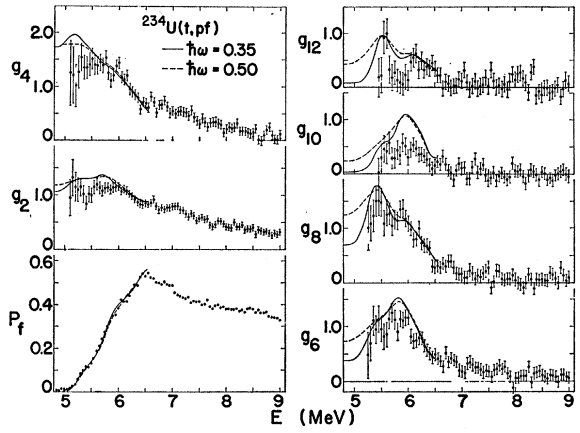

FIG. 11. Fission probability and angular correlation coefficients for the $^{234}U(t,pf)$ reaction. Curves represent fits to the data with assumed barrier penetrability characterized by $\hbar\omega=0.50$ and 0.35 MeV with a microscopic model described in the text.

which, coupled with the target spin I_0, gives a final state J which undergoes fission through a transition state with projection K. The coefficients are given by[5]

$$g_L(jJI_0K)=(2L+1)(LJ0K/JK)\times(Lj0\tfrac{1}{2}/j\tfrac{1}{2})W(LjJI_0jJ)[(2j+1)(2J+1)]^{1/2}.$$

For fission through a particular transition state $(J^\pi K)$, the coefficients are given by

$$g_L(J^\pi K)=\sum_{j=|J-I_0|}^{J+I_0} g_L(jJI_0K)\sigma(j^\pi)/\sum\sigma(j^\pi).$$

For the (t,p) reaction on a spin-0 target with a spin-0 transfer, the expressions simplify to

$$g_L(J^\pi K)=(2L+1)(LJ0K/JK)(LJ00/J0).$$

The contributions from different transition states with the same J^π can now be averaged giving

$$g_L(E^*J^\pi)=\sum_i g_L(J^\pi K_i)\langle\Gamma_f(E^*J^\pi K_i)\rangle/\sum_i\langle\Gamma_f(E^*J^\pi K_i)\rangle,$$

where the summation is taken over all the transition states with the appropriate J^π. The final coefficients for comparison with experiment are obtained by averaging over all states:

$$g_L(E^*)=\sum_{J^\pi} g_L(E^*J^\pi)N(J^\pi)/\sum_{J^\pi}N(J^\pi).$$

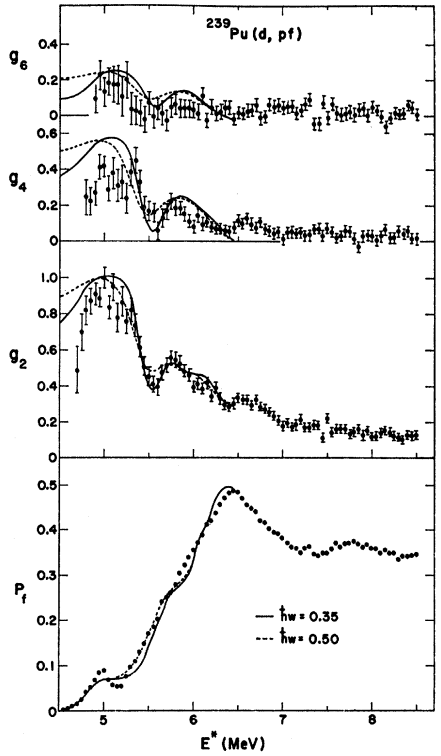

FIG. 12. Fission probability and angular correlation coefficients for the $^{239}Pu(d,pf)$ reaction. Curves represent fits to the data with assumed barrier penetrability characterized by $\hbar\omega=0.50$ and 0.35 MeV with a microscopic model described in the text.

With this model, calculations were performed for a series of parameters and various choices for the transition-state spectrum.

C. Comparison of Calculations with Experimental Results

Calculated distributions from the model described in the previous two sections were compared with the experimental results obtained for the four reactions studied. The parameters of the model and the positions of the vibrational bands in the transition-state spectrum were varied to try to obtain a reasonable characterization of the experimental data. Best fits to the experimental data are shown in Figs. 11–14 and the parameters in the fits are summarized in Tables III and IV.

TABLE III. Statistical parameters for best fits to data in the region $E^*<B_n$.

	$^{239}Pu(d,pf)$		$^{234}U(t,pf)$		$^{235}U(d,pf)$		$^{233}U(d,pf)$	
Parameters	Fitted value	Expected value	Fitted value	Expected value	Fitted value	Expected value	Fitted value	Expected value
a (MeV^{-1})	6	27.4[a]	6	28.5[a]	6	28.5[a]	6	26.8[a]
s	2.5	5.5[a]	4.5	5.8[a]	4.5	5.8[a]	8.0	5.5[a]
Γ_γ (eV)[c]	0.6	0.042[b]	0.25	0.042[b]	0.23	0.042[b]	0.15	0.054[b]
P	2.0	···	2.0	···	5.0	···	0.75	···

[a] A. Gilbert and A. G. W. Cameron, Can. J. Phys. 43, 1446 (1965).
[b] H. H. Hennies, Atomic International Report No. NAA-SR-11980, 1967 (unpublished); see also J. R. Stehn *et al.*, Brookhaven National Laboratory Report No. BNL-325, 2nd ed., Suppl. No. 2, 1965 (unpublished).
[c] Fitted values for Γ_γ are obtained by requiring that the level density formula reproduce experimental values for D, from Ref. b above, for the spins excited in s-wave neutron capture.

TABLE IV. Parameters for best fits to data in the region $E^* < B_n$. Positions of transition states.

Parameters	^{239}Pu(d,pf)		^{234}U(t,pf)		^{235}U(d,pf)		^{233}U(d,pf)	
$\hbar\omega$ (MeV)[a]	0.50	0.35	0.50	0.35	0.50	0.35	0.50	0.35
E_R (keV)[a]	3	5	3	5	3	5	3	5
$E^*(K=0^+)$ (MeV)	4.90±0.05	4.85±0.05	5.35±0.05	5.25±0.05	5.35±0.05	5.25±0.05	5.40±0.05	5.30±0.05
$E^*(K=2^+)$ (MeV)	5.45±0.05	5.45±0.05	6.00±0.05	5.90±0.05	6.00±0.05	5.90±0.05	6.10±0.05	6.00±0.05
$E^*(K=4^+)$ (MeV)	5.80±0.10	5.80±0.10	...	...	...	...	...	...
$E^*(K=0^-)$ (MeV)	5.65±0.05	5.65±0.05	5.80±0.05	5.70±0.05	5.80±0.05	5.70±0.05	5.90±0.05	5.80±0.05
$E^*(K=1^-)$ (MeV)	6.10±0.10	6.05±0.10	6.25±0.10	6.20±0.10	6.25±0.10	6.20±0.10	6.40±0.10	6.30±0.10
$E^*(K=2^-)$ (MeV)	6.25±0.10	6.25±0.10	6.40±0.10	6.35±0.10	6.40±0.10	6.35±0.10	6.55±0.10	6.45±0.10

[a] Values of $\hbar\omega$ and E_R were held fixed. Errors in positions of vibrational bands refer to estimated uncertainties for the particular values $\hbar\omega$ and E_R that were used.

The general procedure for fitting the experimental results can be effectively divided into two parts. First, by using reasonable estimates for the statistical parameters (a, s, P, and Γ_γ) the qualitative features of the results can be reproduced by adjusting the positions of the various vibrational bands in the transition-state spectrum and varying $\hbar\omega$ and E_R. This can be done simply from observing the positions of sharp structure in the P_f and g_L distributions and will be discussed in more detail in Appendix I. Then the statistical parameters can be adjusted to give the best quantitative fit to the experimental results. It has been found that these statistical parameters can be varied over wide ranges without materially affecting the conclusions with regard to the transition-state spectrum that is necessary to give a qualitative fit to the experimental data. The influence of the statistical parameters and general reliability of this microscopic model will be discussed in Appendix I.

It can be seen from Figs. 11–14 that the model is capable of giving a reasonable characterization of both the fission probability and the angular correlations. In comparing the model to experimental data, it was found that the requirement of reproducing the positions of structure in both the fission probability and the angular-correlation coefficients was sufficient to eliminate any ambiguities in the assignment of the vibrational bands for ^{239}Pu(d,pf) and ^{234}U(t,pf). The first positive parity vibrational band expected would be the $K=2^+$ γ vibration (the $K=0^+$ β vibration is unbound at the saddle and should not be observed). A series of negative parity bands ($K=0^-$, 1^-, 2^-, 3^-) from Y_3 deformations of a liquid drop are expected to be present. It is expected that vibrational bands arising from Y_4 and Y_5 deformations occur above the range of excitations considered in these calculations,[27] but it may

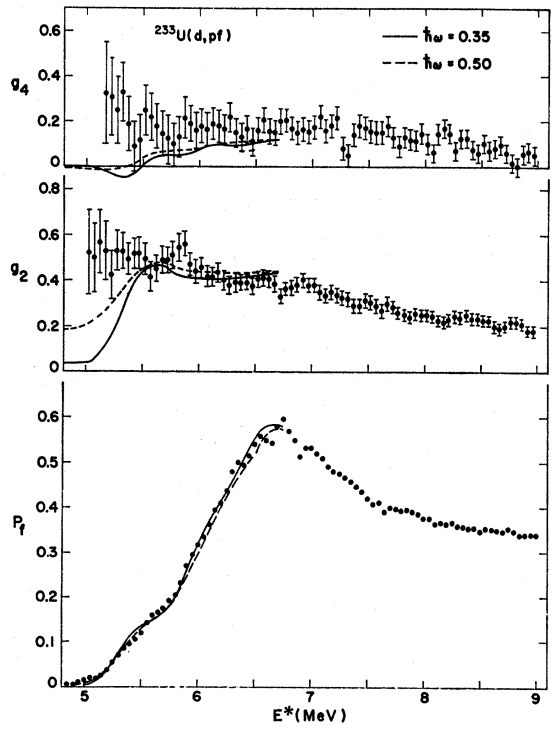

FIG. 13. Fission probability and angular correlation coefficients for the ^{233}U(d,pf) reaction. Curves represent fits to the data with assumed barrier penetrability characterized by $\hbar\omega=0.50$ and 0.35 MeV with a microscopic model described in the text.

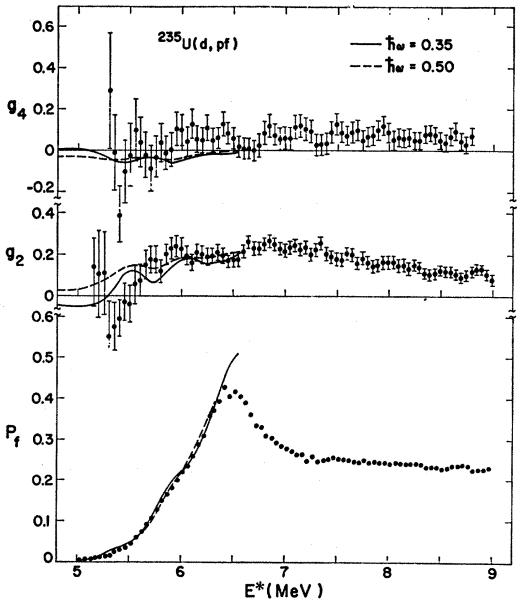

FIG. 14. Fission probability and angular correlation coefficients for the ^{235}U(d,pf) reaction. Curves represent fits to the data with assumed barrier penetrability characterized by $\hbar\omega=0.50$ and 0.35 MeV with a microscopic model described in the text.

[27] J. R. Nix, Ann. Phys. (N.Y.) 41, 52 (1967).

be possible to excite several two-phonon excitations. Possible two-phonon excitations would be the double excitation of the γ vibration to give $K=0^+$ and 4^+ bands and a $K=1^-+K=0^-$ excitation to give a $K=1^+$ band.[28] Thus, it is expected that the first few bands in the transition state spectrum should be $K=2^+$ and $K=0^-$, 1^-, 2^-. At excitations corresponding to approximately twice the lowest band or the sum of the excitations for the first two bands two-phonon excitations could start to appear and the transition-state spectrum become much more complex.

The major ambiguity in the fits to the experimental results was in the values for the barrier penetrability $\hbar\omega$ and the rotational constant E_R. These two parameters have a similar qualitative effect on the predicted distributions. Within the accuracy of the experimental results, it was not possible to uniquely determine both of these parameters. Figures 11–14 show fits with $\hbar\omega=0.5$ MeV, $E_R=3$ keV; and $\hbar\omega=0.35$ MeV, $E_R=5$ keV. These two sets give approximately equivalent fits to the experimental results and also represent approximate expected limits for $\hbar\omega$ and E_R. Thus, from these experiments, significant determinations cannot be made of $\hbar\omega$ and E_R, but the fact that the values used are within reasonable limits tends to support the validity of the model used for the calculations. The uncertainty in $\hbar\omega$ does have a small effect ($\pm\sim 50$ keV) on the estimated positions of the lowest bands because of the fact that as $\hbar\omega$ increases, fission can compete favorably with γ de-excitation at energies farther below the barrier. This effect is automatically accounted for in the microscopic calculations and turns out to be much smaller than previously estimated.[29] The main difference is that previous estimates[29] neglected the width fluctuations in Γ_f.

In the following, the characteristics of the fits to specific sets of experimental results are discussed.

1. $^{239}Pu(d,pf)$

The ^{239}Pu(d,pf) results (Fig. 12) provide the best test of the microscopic model because of the detailed structure observed. The minimum in the value of g_2 at ~ 5.5 MeV can be reproduced only by a $K=2^+$ band at 5.45 MeV followed closely by a $K=0^-$ band at 5.65 MeV. The large step in the fission probability (5.5–5.7 MeV) is due to negative parity states in the $K=0^-$ band becoming available, and the relative magnitude of the first two steps ($K=0^+$ and $K=0^-$) determines the parameter P, which controls the ratio of negative to positive parity states excited. The subsequent rise in g_2 (to ~ 0.55 at $E^*=5.7$ MeV) is also dependent on the value of P. The $K=2^+$ band produces a large change in the g_2 value but has only a small effect on the fission probability. In these results, by fitting both P_f and g_2 the first three bands $K=0^+$, 2^+, 0^- can be uniquely determined. Above 5.7 MeV, the next rise in the fission probability can be reproduced by a $K=1^-$ band at 6.10 MeV which has little effect on g_2, and a $K=2^-$ band at 6.30 MeV produces a decrease in g_2 but only a small effect on P_f. This assignment of vibrational bands reproduces most of the general characteristics of both P_f and g_2 except for the peak in P_f near threshold and the drop in g_2 at ~ 5.9 MeV. A decrease in g_2 at ~ 5.9 MeV can be produced by a $K=4^+$ band at 5.80 MeV but the magnitude is much less than is observed in the experimental results. The threshold peak in P_f cannot be reproduced by any choice of parameters in the present model. Because it occurs at the same excitation energy as a gross structure peak in the (d,p) process (see Fig. 8), the threshold peak may be reflecting a change in the relative (d,p) cross sections which is not allowed in the present model.

2. $^{234}U(t,pf)$

For the ^{234}U(t,pf) results (Fig. 9), the positions of the $K=0^+$ threshold and first $K=0^-$ band are determined primarily by the fission probability distribution. The remaining sequence of bands, $K=2^+$, 1^-, 2^-, provide a reasonable fit to the g_L coefficients up to the neutron binding energy. These results provide a good test of the method used for determining level populations in the model (DWBA cross section plus statistical spin densities). For $K=0^+$ and 0^- bands, there are significant terms in the angular correlations up to $P_{12}(\cos\theta)$, and in the model predictions are sensitive to the $N(J^\pi)$ values used. One prominent feature of the calculations is the large values of g_4, g_8, and g_{12} predicted for $K=0^+$ bands and the large values of g_2, g_6, and g_{10} for $K=0^-$ bands. This effect gives a method of checking the $N(J)$ values used for each parity. The results show that the $K=0^+$ region is reasonably fit for all g_L's, but for the $K=0^-$ band the model gives much larger values for g_{10} than are observed. This indicates that the model is giving too high a population for the high-spin negative-parity levels. A somewhat better fit to $g_6 \rightarrow g_{12}$ could be obtained by allowing different spin cutoff factors for the two parities with the negative parity states having a smaller spin cutoff factor.

3. $^{235}U(d,pf)$

The fits to the ^{235}U(d,pf) results (Fig. 14) were restricted by holding all parameters except P and Γ_γ to the values obtained from the ^{234}U(t,pf) results. With these restrictions, a reasonable fit can be obtained to the fission probability, but a very large value of P is required (practically all the levels excited are of negative parity). These results indicate that the "threshold" observed in earlier experiments[4] was

[28] J. J. Griffin, in *Proceedings of the Symposium on Physics and Chemistry of Fission* (International Atomic Energy Agency, Vienna, 1965), Vol. I, p. 23.

[29] L. N. Usachev, V. A. Pavlinchuk, and N. S. Rabotnov, Zh. Eksperim. i Teor. Fiz. 44, 1950 (1963) [English transl.: Soviet Phys.—JETP 17, 1312 (1963)].

actually due to the $K=0^-$ band and the true threshold ($K=0^+$) was not observed because of the small amount of fission through positive parity levels. The calculations give a reasonable fit to g_2 except for the sharp dip below threshold. This dip has recently been explained[30] as being due to nuclear polarization effects which have not been included in the present model.

4. $^{233}U(d,pf)$

For the ^{233}U(d,pf) results (Fig. 11), the fit was based entirely on the fission probability distribution. A reasonable fit can be obtained with a spectrum of transition states very similar to ^{236}U. However, a deviation between the model and experiment is observed in the region below threshold where the model predicts that g_2 and g_4 should decrease in contradiction to the experimental data. The predicted decrease is a general result of the $\frac{5}{2}^+$ target spin and is observed in ^{235}U(d,pf) for target spin $\frac{7}{2}^-$. A similar effect is observed[31] in very low energy deuteron anisotropies [fission occurs predominantly from (d,pf) reaction] where ^{235}U shows $W(0°/90°)<1$ for 6-MeV deuterons, but ^{233}U still gives $W(0°/90°)>1$.

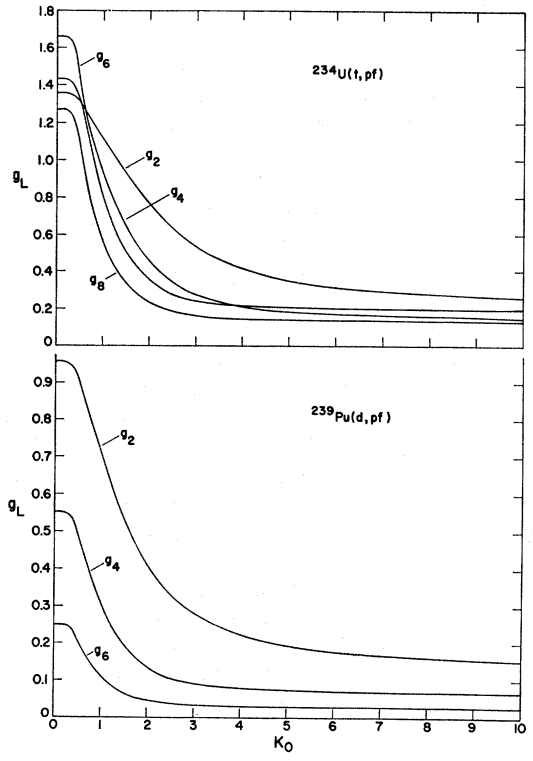

FIG. 15 Dependence of g_L values on K_0 from the statistical model described in the text for ^{234}U(t,pf) and ^{239}Pu(d,pf).

[30] R. Vandenbosch, K. L. Wolf, J. Unik, C. Stephan, and J. R. Huizenga, Phys. Rev. Letters **19**, 1138 (1967).

[31] Yu. A. Nemilov, Yu. A. Seiliskii, S. M. Solov'ev, and V. P. Eismont, Yadern. Fiz. **2**, 460 (1965) [English transl.: Soviet J. Nucl. Phys. **2**, 330 (1965)].

V. ANALYSIS OF RESULTS: STATISTICAL ANALYSIS $E^*>B_n$

A. Method

For these nuclei at the neutron binding energy, the excitation is large enough so that many vibrational bands are contributing to the fission process, and analysis in terms of a detailed model becomes meaningless because of the ambiguities in the assignment of specific bands. In the excitation energy region above B_n, a simple statistical model has been used to analyze the results. This model is essentially the same as that used previously[5] for ^{239}Pu(d,pf) data. In this model, it is assumed that there is a statistical distribution of K values available for fission which is given by

$$\rho(K)=\exp\left(-\frac{K^2}{2K_0{}^2}\right).$$

Then, using the distribution of states excited by the direct reaction, $N(J^\pi)$, from the fits in the preceding section, values for g_L can be calculated for the (d,pf) and (t,pf) reactions. The results of these calculations as a function of K_0 are shown in Fig. 15 for the ^{239}Pu(d,pf) and ^{234}U(t,pf) reactions.

B. Analysis of Results—Determination of Pairing Gap in the Transition-State Spectrum

Figure 16 shows the results obtained for K_0 from the statistical analysis of g_2 for the ^{239}Pu(d,pf) reaction

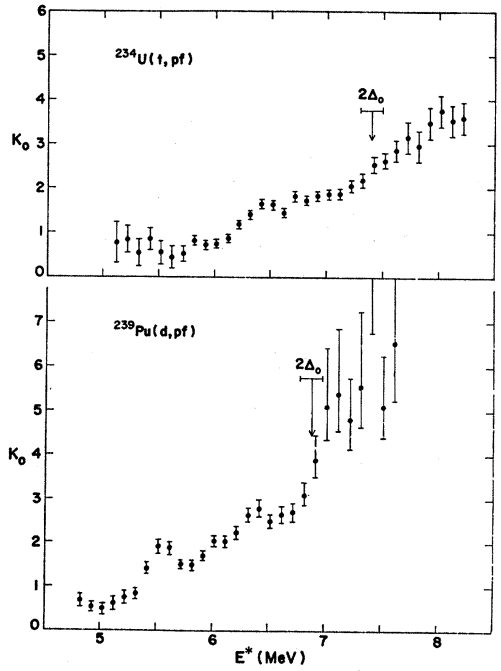

FIG. 16. Dependence of K_0 on E^* from the statistical analysis of the ^{234}U(t,pf) and ^{239}Pu(d,pf) results. The positions determined for the pairing gaps ($2\Delta_0$) are indicated.

and the average of g_2 and g_4 for the ^{234}U(t,pf) reaction. The results show an increase in K_0 from $\sim$2.5 to $\sim$5 at $E^*=6.88\pm0.10$ MeV for ^{239}Pu(d,pf), and an increase in K_0 from $\sim$1.8 to $\sim$3.5 at $E^*=7.40\pm0.10$ MeV for ^{234}U(t,pf). These changes in K_0 correspond to a definite step in g_2 for $^{239}(d,pf)$ (Fig. 12) and a sharp change in the anisotropy for the ^{234}U(t,pf) results shown in Fig. 17. The absolute values obtained for K_0 from the data are uncertain because of the uncertainties in $N(J^\pi)$. However, the magnitude of the change observed in K_0 is consistent with the change expected when the excitation energy exceeds the energy $(2\Delta_0)$ required to excite two-quasiparticle states. If these steps are interpreted as the pairing gap for the nucleus at its saddle-point deformation, then values are obtained $2\Delta_0=2.10\pm0.15$ MeV for ^{236}U and $2\Delta_0=1.98\pm0.15$ MeV for ^{240}Pu. For stable deformations, values of the pairing gap for neutrons and protons have been reported[32] as $2\Delta_n=1.06$ MeV, $2\Delta_p=1.48$ MeV for ^{240}Pu, and $2\Delta_n=1.38$ MeV, $2\Delta_p=1.84$ MeV for ^{236}U. Thus, the present results show that the pairing gap at the saddle-point deformation is significantly larger than at the stable deformation. The present results agree, to within the statistical accuracy, with the previous data as is shown in Fig. 18, but the estimate $2\Delta_0=1.98\pm0.15$ for ^{240}Pu is considerably less than the value $2.6_{-0.45}^{+0.21}$ quoted previously.[5]

An additional check is available on the reliability of this assignment of the pairing gap in the transition-state spectrum. If the pairing gap at the saddle-point deformation, Δ_s, is larger than for the nucleus at its stable shape, Δ_g, then there should be a systematic difference $\Delta_s-\Delta_g$ between the fission thresholds for

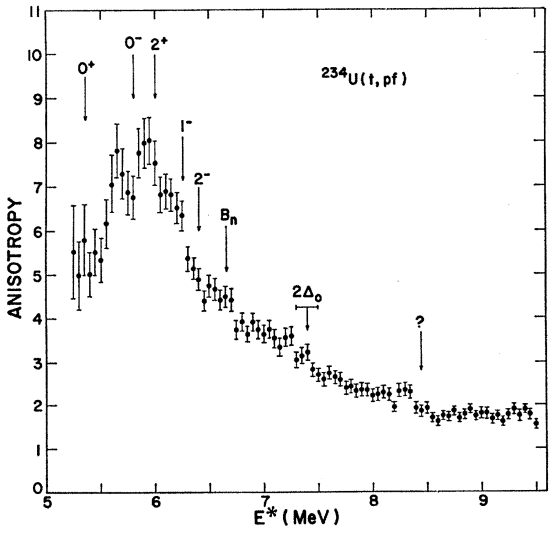

FIG. 17. Measured anisotropies for the ^{234}U(t,pf) reactions. Anisotropy is obtained from the ratio of experimental coincidence rate for a sum of detectors at center-of-mass angles of $\sim$0° and $\sim$5° to the rate for a sum of detectors at $\sim$83° and $\sim$87°.

[32] P. E. Nemirovsky and Yu. V. Adamchuk, Nucl. Phys. **39**, 551 (1962).

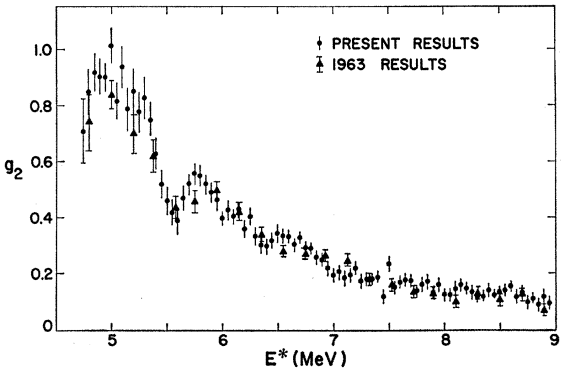

FIG. 18. Comparison of the present results for g_2 from the ^{239}Pu(d,pf) reaction with previous results from Ref. 5.

even-even nuclei and odd-neutron, even-proton nuclei. From the present measurements, thresholds of 5.30 and 5.35 MeV have been determined for ^{234}U and ^{236}U, respectively. Loveland *et al.*[16] have determined the lowest transition state in ^{235}U as being a $\frac{3}{2}^+$ state at a neutron energy of 0.39 MeV. Using a neutron binding energy of 5.305 MeV from measured Q values gives a threshold of $E^*=5.695$. These values give an odd-even threshold difference $\Delta_s-\Delta_g=0.38\pm0.1$ MeV. For $2\Delta_g=1.38$ MeV a pairing gap $2\Delta_s=2.14\pm0.20$ MeV is obtained. This value is in good agreement with the value 2.10 ± 0.15 obtained above and indicates that this is the gap appropriate for the neutron spectrum.

The estimated uncertainties in $2\Delta_s$ include the uncertainty in estimating the position of the lowest $K=0^+$ state in the transition-state spectrum within the framework of the present simplified model. However, these estimated uncertainties do not include any systematic errors which might arise due to gross inadequacies in the present model. A discussion of the possible inadequacies in the present model is given in Appendix I.

In the ^{234}U(t,pf) anisotropy, there is an additional sharp change which occurs at $E^*\sim8.4$ MeV corresponding to an excitation energy of 3.1 MeV in the transition-state spectrum. If the step at 2.1 MeV corresponds to the pairing gap for neutrons, then the next observed step at 3.1 MeV could be the pairing gap for proton states. This identification would give neutron and proton pairing gaps at the saddle-point deformation (2.1 and 3.1 MeV, respectively) which are increased by approximately the same percentage over the neutron and proton pairing gaps for the stable deformation (1.38 and 1.84 MeV, respectively).

VI. SUMMARY AND DISCUSSION

In the preceding sections, the results from (d,pf) and (t,pf) correlation experiments have been presented and compared to calculations from a simple model in an attempt to determine the positions and character of the low-lying vibrational bands in the transition-state

spectrum. At higher excitation energies, the results have been analyzed assuming a statistical distribution of states available in the transition-state spectrum. This analysis resulted in the possible identification of the pairing gap in the transition-state spectrum for ^{236}U and ^{240}Pu.

In spite of the simplified assumptions and the inadequacies (see Appendix I) of the model, a good characterization of the experimental results is obtained from the calculations. Within the general framework of the model, the positions of the $K=0^+$, 2^+, and 0^- vibrational bands are determined uniquely for ^{240}Pu and ^{236}U, and for ^{234}U a very similar level scheme gives a good fit to the fission probability. At higher excitations, $K=1^-$ and 2^- bands are needed to fit the results. At excitation energies above the $K=2^+$ band, the experimental results have become relatively insensitive to the addition of further positive parity bands and a similar situation arises for negative parity bands above the $K=2^-$ band. Schematic diagrams of the vibrational bands identified in the transition-state spectra of ^{234}U, ^{236}U, and ^{240}Pu are shown in Figs. 19 and 20. These results represent the first quantitative determination of the thresholds and low-lying vibrational bands in the transition-state spectrum of an even-even nucleus.

For ^{240}Pu, the positions of the $K=0^-$ and 1^- bands can be compared to values inferred from recent photofission experiments.[33] The present results give positions of 5.65±0.10 and 6.10±0.10 MeV for the lowest 1^- ($K=0$) and 1^- ($K=1$) transition states, respectively. These values are larger than the values 5.2 MeV for the 1^- ($K=0$) state and 5.7 MeV for the 1^- ($K=1$) state from the photofission results.[33] Both results give the same energy difference between the two 1^- levels but the (d,pf) results give absolute positions that are approximately 0.5 MeV higher than the photofission results.[33] The significance of this discrepancy between the two experiments is difficult to assess because estimates of the errors in the positions determined in the photofission experiments are not given and the analysis of these data is complicated by having to unfold contributions from γ rays with many different energies in a bremsstrahlung spectrum.

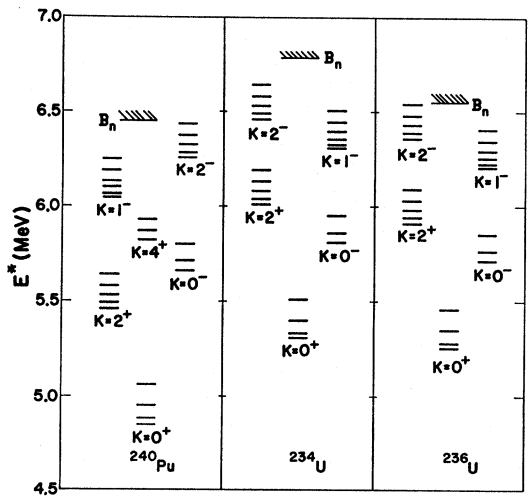

FIG. 19. A schematic diagram of the transition-state spectra for ^{240}Pu, ^{234}U, and ^{236}U from the fits to the experimental results with $\hbar\omega=0.35$ MeV, $E_R=5$ keV. The positions and uncertainties for the vibrational bands are also tabulated in Table IV.

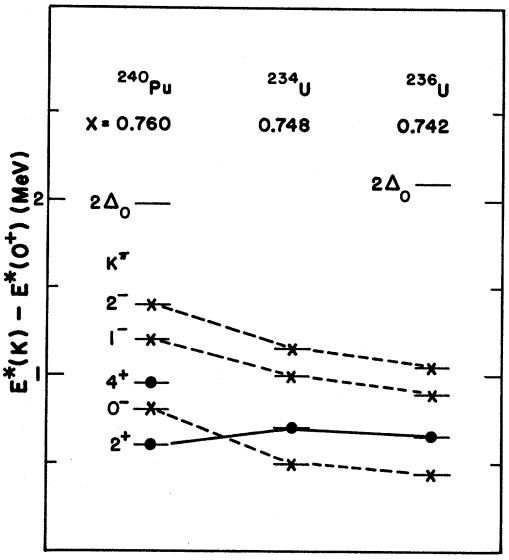

FIG. 20. Positions of the bands in the transition-state spectra relative to the $K=0^+$ threshold from the fits to the experimental results with $\hbar\omega=0.35$ MeV and $E_R=5$ keV. Values of $x=(Z^2/A)/48.4$ are included for each nucleus.

The positions of some of the low-lying vibrational bands in the transition-state spectrum can be compared both to their positions at stable nuclear deformation and to liquid-drop calculations for the saddle-point deformation. Changes in the vibrational energies between the stable and saddle-point deformations can arise from two general effects. First, in the liquid-drop model, a change in vibrational energies is expected because of a change in the nuclear shape. In addition, the actual vibrational energies are perturbed from liquid-drop estimates by single-particle effects, and these perturbations are expected to be larger for the smaller stable deformations. For example, at the stable deformation, the $K=2^+$ "γ vibration" has been observed[34] at 0.92 MeV for ^{234}U and at 1.03 MeV for ^{240}Pu, as compared to values at the saddle-point deformation of 0.70 MeV for ^{234}U and 0.55 MeV for ^{240}Pu. In a liquid-drop model, one would expect[3] the energy of the $K=2^+$ band to increase with increasing deformation because of the decreasing cross sec-

[33] N. S. Rabotnov, G. N. Smirenkin, A. S. Soldatov, L. N. Usachev, S. P. Kapitsa, and Yu. M. Tsipenyuk, in *Proceedings of the Symposium on Physics and Chemistry of Fission* (International Atomic Energy Agency, Vienna, 1965), Vol. I, p. 135 [English transl.: Argonne National Laboratory ANL-Trans-245].

[34] Earl K. Hyde, University of California Lawrence Radiation Laboratory Report No. UCRL-8783, rev., 1963 (unpublished).

TABLE V. A comparison of calculated positions for the negative parity bands for the nucleus at its equilibrium deformation with measured values at the saddle-point deformation.

	$K^\pi=0^-$		$K^\pi=1^-$		$K^\pi=2^-$	
Nucleus	Calc.[a]	Expt.[b]	Calc.[a]	Expt.[b]	Calc.[a]	Expt.[b]
^{234}U	0.71	0.55±0.1	0.94	0.90±0.1	1.12	1.05±0.1
^{236}U	0.74	0.55±0.1	1.01	0.90±0.1	1.24	1.05±0.1
^{240}Pu	0.65	0.75±0.1	1.04	1.20±0.1	1.52	1.35±0.1

[a] For nucleus at equilibrium deformation from Ref. 35.
[b] For nucleus at saddle-point deformation.

tional area. Thus, these results suggest that at stable deformations the $K=2^+$ energy of $\sim$1 MeV may be strongly influenced by single-particle effects. The energies of the negative parity bands for $K=0^-$, 1^-, and 2^- can be compared to theoretical calculations[35] of the positions of these bands at stable deformations for the nuclei of interest. These comparisons are shown in Table V and they indicate that there is very little change in the energies of the negative parity vibrations as the nucleus is deformed from its equilibrium deformation to the saddle-point deformation.

In addition, it is possible to compare some of the characteristics of the experimental transition-state spectrum to the theoretical calculations of Nix[27] for an idealized irrotational liquid drop. For an irrotational liquid drop, Nix has calculated the characteristic frequencies $\hbar\omega_2$ (equivalent to our $\hbar\omega$) and $\hbar\omega_3$ (position of the $K=0^-$ band). For real nuclei, it is well known that the effective masses associated with vibrational frequencies are several times greater than those calculated from an irrotational model. If it is assumed that the stiffness potential energy of a very deformed shape is correctly given by the liquid-drop model, then a comparison between measured and calculated values of $\hbar\omega_2$ and $\hbar\omega_3$ can be used to estimate the effective masses. Using this approach, Nix[27] concludes that for $\hbar\omega_2$, the effective mass is $\sim$2.8 times the irrotational value. This conclusion is reached from the fact that $\hbar\omega_2$ determined from spontaneous fission half-lives is 0.6 times the calculated value. Using $(Z^2/A)_{\text{critical}}=48.4$ and $M_{\text{effective}}=2.8\times M_{\text{irrotational}}$, values of $\hbar\omega_2$ from these calculations would be 0.36 MeV for ^{236}U and 0.40 MeV for ^{240}Pu. These values are consistent with the range $0.35\leq\hbar\omega\leq0.50$ MeV determined from the present experiment. This same prescription gives values $\hbar\omega_3=0.8$ MeV for ^{236}U and $\hbar\omega_3=0.9$ MeV for ^{240}Pu, as compared to positions for the $K=0^-$ band $[E^*(K=0^-)-E^*(K=0^+)]$ from the fits to the experimental data of 0.45±0.05 MeV for ^{236}U and 0.75±0.05 MeV for ^{240}Pu. In both cases, the values are lower than calculations for an effective mass of $2.8\times M_{\text{irrotational}}$. The trend of an increase in energy of the $K=0^-$ vibration with increasing Z^2/A is as predicted in the liquid-drop calculations, but the rate of increase is greater in the experimental results than in the theoretical calculations. Again assuming that the stiffness is given accurately by the liquid-drop calculations, these results would indicate an effective mass of $(9\pm2.5)\times M_{\text{irrotational}}$ for ^{236}U and $(4\pm0.6)\times M_{\text{irrotational}}$ for ^{240}Pu.

On the basis of a more approximate irrotational liquid-drop model, Griffin[28] has estimated the relative spacing of the $K=1^-$ and $K=0^-$ vibrations. This calculation yielded a value for $R=[E^*(K=1^-)-E^*(K=1^-)]/[E^*(K=0^-)-E^*(K=0^+)]$ of $\sim$0.25. This value is considerably less than the present experimental values for R of 1±0.35 for ^{236}U and 0.6±0.2 for ^{240}Pu.

From the statistical analysis of the data above the neutron binding energy and the odd-even fluctuation in fission thresholds, the neutron pairing gap is identified in ^{234}U and ^{240}Pu at $\sim$2.0 MeV, which is about 50% higher than observed for these nuclei at their stable deformations. This result is consistent with theoretical calculations[36] which indicate that pairing is a finite-nucleus effect and should depend on the nuclear surface-to-volume ratio. Recent calculations[37] of this effect, assuming that the pairing force varies proportionally to the magnitude of the nuclear surface, have yielded a value $2\Delta_n\sim1.8$ MeV for ^{240}Pu, which is in agreement with the experimental value of 1.98±0.15 MeV. Similar experimental results are also obtained for ^{210}Po and ^{211}Po, where evidence[38] has been presented for a pairing energy of $\sim$4 MeV at the saddle-point deformation. In this case, the saddle-point deformation is much larger than for the more fissionable U and Pu isotopes.

ACKNOWLEDGMENTS

We gratefully acknowledge helpful discussions with P. Axel, J. J. Griffin, A. K. Kerman, B. R. Mottelson, and J. R. Nix on the interpretation of these results. We are indebted to Mrs. Judith C. Gursky and J. G. Povelites for preparing the targets used in these experiments. We are grateful to J. S. Levin and M. P. Kellogg for developing the computer programs used in the on-line data reduction.

APPENDIX

In this Appendix the adequacy of the present simplified model for describing the direct-reaction fission process will be discussed from two aspects. First, the ambiguities in the assignments of transition-state spectra due to the statistical approximations in the model will be discussed. It is shown that the positions and character of the low-lying vibrational transition states can be determined from qualitative characteristics of the experimental results and the identifi-

[35] L. A. Malov, V. G. Soloviev, and P. Vogel, Phys. Letters **22**, 441 (1966).

[36] R. C. Kennedy, L. Wilets, and E. M. Henley, Phys. Rev. Letters **12**, 36 (1964); R. C. Kennedy, Phys. Rev. **144**, 804 (1966).

[37] W. Stepien and Z. Szymanski, Phys. Letters **26B**, 181 (1968).

[38] L. G. Moretto, R. C. Gatti, J. R. Huizenga, and J. O. Rasmussen, Bull. Am. Phys. Soc. **12**, 521 (1967).

cations are not highly sensitive to reasonable changes in the parameters used for the description of the statistical aspects of the formation and decay processes. In the second part of this Appendix the values obtained for the statistical parameters from fits to the experimental results will be discussed and comparisons made with results from studies of individual neutron resonances. Comparisons of the parameters with expected values gives some information on possible improvements to the model and on the areas in which the general formulation of a simple channel theory of fission may be inadequate.

A. Adequacy of Model for Determining Transition-State Spectra

In many cases the parameters obtained from fits to the experimental data are somewhat different from the values which would be expected from other considerations. These differences are due in most cases to the simplifying assumptions used in the model and will be discussed in detail below. In Fig. 21 the general effects of changes in the statistical parameters on the calculated distributions from the model are illustrated. In all cases the solid curves represent the best fit to the ^{239}Pu(d,pf) results shown in Fig. 12 and other curves show the effect of large changes in the parameters of the model. Figure 21(B) shows the effects of changing the level density parameter a by a factor of 4 or the value of Γ_γ by a factor of 10. In both cases the calculated g_2 distribution is not significantly affected. Changes in Γ_γ affect the normalization and the level density parameter affects the over-all slope of the P_f distribution. Figure 21(C) shows results of changing P and s by a factor of 2. These parameters affect both the g_2 and P_f distributions. However, Figs. 21(B) and 21(C) illustrate quite clearly that the character and positions of structure in the g_2 and P_f distributions are determined by the properties of the transition-state spectrum and are not qualitatively affected by changes in the statistical parameters a, Γ_γ, P, and s. From Figs. 21(B) and 21(C) it can be seen that large changes in these parameters give only small changes in the positions of the prominent structure in the calculated distributions (e.g., the center of the large drop in g_2 on the half-rise positions for thresholds in P_f). These calculations indicate that within the framework of the present model there is an uncertainty of $\sim\pm 0.1$ MeV in the determination of the positions of the first few vibrational bands in the transition-state spectrum.

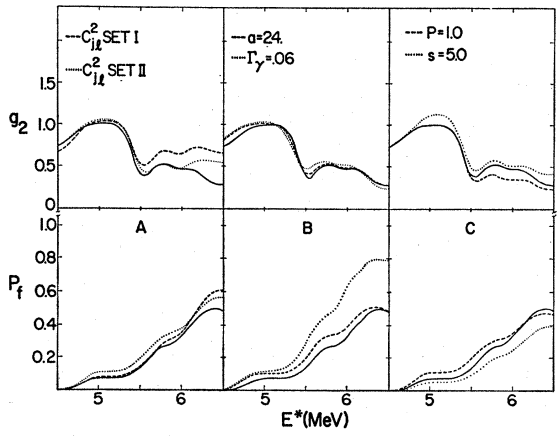

FIG. 21. Results of varying parameters in the model calculations for the ^{239}Pu(d,pf) results. In all cases the solid curves show the best fit from Fig. 12. (A) The states populated are taken from single-particle calculations as described in the text. (B) Shows the results of changing the level density parameter a by a factor of 4 and the γ-ray width Γ_γ by a factor of 10. (C) Shows the effect of changing P and the spin cutoff factor s by a factor of 2.

Another simplifying assumption made in the model calculations is that the angular momentum distribution is of a statistical form with an exponential spin cutoff factor. To test the sensitivity of the calculations to this assumption an alternative approach was used in which it was assumed that the (d,p) process populates a distribution of states which is determined by the spectroscopic factors C_{jl}^2 predicted[39] for the single-particle bands in the appropriate excitation energy region. This alternative approach effectively assumed that the single-particle strength from these bands is spread uniformly throughout the region of interest and determines the character of the states excited by the (d,p) reaction. Figure 21(A) illustrates the results from the alternative approach to the formation process. Two sets of single-particle bands were used.[40] Set I includes a cluster of bands predicted in the region between 1.5 and 2.5 MeV below the neutron binding energy. Set II includes these same bands and in addition all of the other bands predicted up to the neutron binding energy. The results in Fig. 21(A) show that as the number of single-particle bands included in the calculations is increased in going from set I to set II the predicted distributions approach more closely the model calculations using the statistical assumption. The only major difference between the set-II calculations and the original model calculations is in the region 6.0–6.5 MeV in the g_2 distribution. This difference comes from the fact that the negative parity cross section is dominated by the lowest members of the $N=7$ oscillator shell which have strength predominantly in the high-spin members. The addition of contributions from higher $N=7$ states would tend to bring the results from the alternative calculation into better agreement with the result using the statistical assumption. These calculations show that the statistical assumption is capable of reproducing the results from

[39] The predictions for single-particle bands were obtained from the code of E. Rost, Phys. Letters **26B**, 184 (1968); Phys. Rev. **154**, 994 (1967).

[40] The single-particle bands used in the calculation are as follows (notation: spin-parity, predicted energy in MeV relative to neutron binding energy): Set I—$\frac{1}{2}^+$, -2.02; $\frac{5}{2}^+$, -2.21; $\frac{11}{2}^+$, -2.53; $\frac{1}{2}^-$, -1.62; $\frac{1}{2}^-$, -2.19; $\frac{3}{2}^-$, -1.88; $\frac{13}{2}^-$, -1.78: Set II contains all of the previous bands and in addition—$\frac{1}{2}^+$, -0.38; $\frac{3}{2}^+$, -2.64; $\frac{3}{2}^+$, $+0.06$; $\frac{5}{2}^+$, -1.07; $\frac{7}{2}^+$, -0.06; $\frac{9}{2}^+$, -2.81; $\frac{1}{2}^-$, $+0.23$; $\frac{3}{2}^-$, -1.03; $\frac{5}{2}^-$, -0.16; $\frac{5}{2}^-$, -1.15; $\frac{7}{2}^-$, $+0.00$; $\frac{15}{2}^-$, $+0.18$.

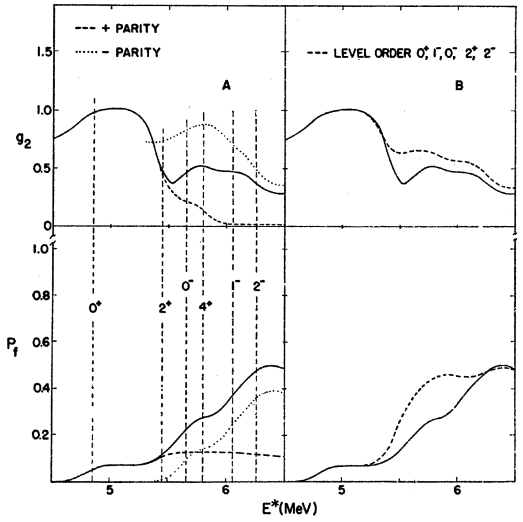

FIG. 22. Results of calculations to test the uniqueness of the transition-state assignments from ^{240}Pu. The solid curves show the best fit from Fig. 12 for ^{239}Pu(d,pf). (A) Shows the positive and negative parity components for the best fit. (B) Shows an attempt to fit the results with a level ordering 0^+, 1^-, 0^-, 2^+, 2^- for the transition-state spectrum.

a sum over contributions from a large number of single-particle bands.

Figure 22 illustrates the sensitivity of the model calculations to the level ordering assumed for the transition-state spectrum for ^{240}Pu. In Fig. 22(A) the separate contributions of positive and negative parity states to the P_f and g_2 distributions are shown for the best fit. Because the nuclei considered are even-even there are only a few vibrational bands which can occur in the transition-state spectrum at low excitations. Figure 22(B) represents an attempt to find an alternative level ordering to fit the ^{239}Pu(d,pf) results. The only other acceptable sequence that could produce a dip in g_2 at $\sim$5.5 MeV would be 0^+, 1^-, 0^-. It is seen in Fig. 22(B) that this choice gives a poorer fit for g_2 and a prediction for P_f that is very different from the experimental results. Even if the sequence is assumed as 0^+, 2^-, 0^- a fit cannot be obtained to the fission probability and in any case it is extremely unlikely that the $K=2$ band would be the first negative parity band encountered in the transition-state spectrum. These results illustrate the uniqueness of the level order determined within the framework of the present model for ^{240}Pu. For ^{236}U from the ^{234}U(t,pf) reaction the ordering of the vibrational bands is similarly well determined. For ^{233}U(d,pf) only the fission probabilities are used in the fits so that the reliability of the determinations is significantly less. However, the results indicate that the ^{233}U(d,pf) results can be reproduced with a level spectrum for ^{234}U that is very similar to the spectrum for ^{236}U.

B. Statistical Parameters from Model Fits

Figures 21(B) and 21(C) illustrate the sensitivity of the calculations to the statistical parameters used in the model. In these plots one can also see the interdependencies of the various parameters. Because of the interactions between various parameters, the sets used in these fits may not be unique. For example, changes in the parameter P and the level density parameter a have very similar effects on the fission probability distributions. In addition there are expected effects that are not included in the present model but which can be simulated by adjustments in the parameters obtained from fits to the data. For example, an energy dependence in the formation cross sections or in Γ_γ can be approximately simulated by a change in the value of the level density parameter or the parameter P. A first-order angular momentum dependence for Γ_γ is supplied by the spin cutoff parameter s. Thus, some of the differences between parameters obtained from the fits to the present results and the values that would be expected from other considerations can be explained in terms of deficiencies in the details of the present simplified model. The deviations of the values obtained for a and s from the systematics of Gilbert and Cameron[25] are not considered significant and are probably due to the oversimplification of the model.

A more serious discrepancy occurs for Γ_γ between the model fits and measured values obtained from neutron resonance experiments.[41] The model fits are not sensitive directly to Γ_γ but rather to $\langle\Gamma_f\rangle/\Gamma_\gamma$ so that the results shown in Table III can be equivalently interpreted as indicating abnormally large values of Γ_γ or $\langle\Gamma_f\rangle$ values that are small compared to those calculated in the present model. For the compound nucleus ^{236}U, a detailed comparison can be made between the present data and results obtained from analysis of neutron resonance data. From the evaluations of Hennies[41] a value of 0.67 is recommended for the quantity $\sigma_f/(\sigma_f+\sigma_c)$ integrated over the entire resonance region. This should be compared to 0.59 ± 0.06 for the value of P_f at the neutron binding energy averaged for 3^- and 4^- states from the fit to the present data. This comparison suggests that the average values $\langle\Gamma_f\rangle/\Gamma_\gamma$ for 3^- and 4^- states are in reasonable agreement for the two different types of experiment. If it is further assumed that the values of Γ_γ and $\bar{D}$ from the neutron resonance measurements are correct then a standard channel analysis of either the neutron resonance results or the present direct-reaction fission results indicates an effective number of open channels for 3^- and 4^- states of $\sim$0.5. In contrast, the fluctuations in fission widths from neutron resonance experiments and the occurrence of structure in the direct-reaction fission experiments indicate that 2 to 3 channels are contributing to the fission process for both 3^- and 4^- states. These results suggest that there may be contributions from 2 to 3 transition states with the penetrability for each state being roughly equal and consider-

[41] H. H. Hennies, Atomic International Report NAA-SR-11980, 1967 (unpublished); see also J. R. Stehn *et al.*, Brookhaven National Laboratory Report No. BNL-325, 2nd ed., Suppl. No. 2, 1965 (unpublished).

ably less than one. However, for a parabolic fission barrier this would require a much larger value of $\hbar\omega$ and would be inconsistent with the observation of any structure in the direct-reaction fission process. The above dilemma seems to point to a basic flaw in the simple channel model of the fission process which has been used here and in most previous work. The problem may well be in the parabolic shape assumed for the fission barrier. Recent calculations[42] have shown that single-particle effects strongly influence the barrier shapes. Measurements of fission isomers[43] and intermediate resonances[44] in the sub-barrier fission of even-even targets indicate that the barriers may even be double peaked. Detailed penetrability calculations have not been performed for the variety of barrier shapes now postulated but it does seem possible that these barriers might give a sharp initial rise in the penetrability with a subsequently slow increase to a penetrability of unity. Such a barrier penetrability function could make all of the information from both neutron resonance and direct-reaction fission experiments internally consistent.

For the compound system ^{234}U, the neutron resonance results[45] give an average fission width ($\sim$0.34 eV) in good agreement with calculated fission widths from the (d,pf) fits (0.55 eV for 2^+ states and 0.28 eV for 3^+ states) and the value of Γ_γ in the (d,pf) fits is approximately a factor of 3 greater than the experimental value from resonance results. By allowing a reduced penetrability for negative parity states as is observed in ^{236}U, and suitably adjusting Γ_γ and P, the neutron resonance results and the fits to the (d,pf) results can be made internally consistent. This would lead to the conclusion that ^{234}U and ^{236}U are very similar but that possibly the fission barrier has a different shape for positive and negative parities. If the shape of the barrier is being strongly influenced by single-particle effects, this is not an unreasonable hypothesis.

For ^{240}Pu the model fits require an even larger value of Γ_γ possibly indicating a further reduced fission penetrability. In this case, it is not possible to make meaningful comparisons to the neutron resonance results because these experiments obtain only very limited information about the 0^+ states and the (d,pf) fits do not include fission through the 1^+ states.

The other major puzzle in the parameters obtained from the fits to the direct-reaction fission results is the values obtained for the parameter P, giving the ratio of fission through negative relative to positive parity states. The fits indicate a preponderance of fission through negative parity states for ^{240}Pu and ^{236}U with roughly equal contributions for ^{234}U. If fission is inhibited for negative parity states as suggested above, then the relative formation of negative parity states could be even greater than suggested by the values of P from the fits. Very little is known about the ratio of single-particle strength for negative and positive parities but because of the difference in parity for the targets ^{235}U($\frac{5}{2}^+$) and ^{235}U($\frac{7}{2}^-$) it was expected that the value of P for the ^{233}U(d,pf) reaction should be roughly the inverse of the value for the ^{235}U(d,pf) reaction. From Table III it can be seen that this is not the case. It may be that the value of P is slowly varying as a function of excitation energy or that the values observed represent compensations for other excitation energy dependences that are not included in the present model. A more complete understanding of this problem awaits a more thorough investigation of both the direct-reaction and the fission decay processes.

[42] V. M. Strutinski, Nucl. Phys. **A95**, 420 (1967).

[43] G. N. Flerov, A. A. Pleve, S. M. Polikanov, S. P. Tretyakova, N. Martalogu, D. Poenaru, M. Sezoni, I. Vilcov, and N. Vilcov, Nucl. Phys. **A97**, 444 (1967); G. N. Flerov, A. A. Pleve, S. M. Polikanov, S. P. Tretyakova, I. Boca, M. Sezoni, I. Vilcov, N. Vilcov, *ibid.* **A102**, 443 (1967); S. Bjørnholm, J. Borggreen, L. Westgaard, and V. A. Karnaukhov, *ibid.* **A95**, 513 (1967); J. Borggreen, Y. P. Gangrsky, G. Sletten, and S. Bjørnholm, Phys. Letters **25B**, 402 (1967).

[44] A. Fubini, J. Blons, A. Michaudon, and D. Paya, Phys. Rev. Letters **20**, 1373 (1968); E. Migneco and J. P. Theobold, Nucl. Phys. **A112**, 603 (1968).

[45] D. W. Bergen and M. G. Silbert, Phys. Rev. **166**, 1178 (1968).